Geminin facilitates FoxO3 deacetylation to promote breast cancer cell metastasis

Lei Zhang,[1] Meizhen Cai,[1] Zhicheng Gong,[1] Bingchang Zhang,[1] Yuanpei Li,[1] Li Guan,[1] Xiaonan Hou,[1] Qing Li,[1] Gang Liu,[2] Zengfu Xue,[3] Muh-hua Yang,[4] Jing Ye,[5] Y. Eugene Chin,[6] and Han You[1]

[1]State Key Laboratory of Cellular Stress Biology, Innovation Center for Cell Signaling Network, School of Life Sciences, and [2]State Key Laboratory of Molecular Vaccinology and Molecular Diagnostics Center for Molecular Imaging and Translational Medicine School of Public Health, Xiamen University, Xiamen, Fujian, China. [3]Xiamen Cancer Center, The First Affiliated Hospital of Xiamen University, Xiamen, Fujian, China. [4]Institute of Clinical Medicine, National Yang-Ming University, Taipei, Taiwan. [5]Department of Pathology, Xijing Hospital, Fourth Military Medical University, Xi'an, Shanxi, China. [6]Key Laboratory of Stem Cell Biology, Institute of Health Sciences, Shanghai Institutes for Biological Sciences, Chinese Academy of Sciences–Jiaotong University School of Medicine, Shanghai, China.

Geminin expression is essential for embryonic development and the maintenance of chromosomal integrity. In spite of this protective role, geminin is also frequently overexpressed in human cancers and the molecular mechanisms underlying its role in tumor progression remain unclear. The histone deacetylase HDAC3 modulates transcription factors to activate or suppress transcription. Little is known about how HDAC3 specifies substrates for modulation among highly homologous transcription factor family members. Here, we have demonstrated that geminin selectively couples the transcription factor forkhead box O3 (FoxO3) to HDAC3, thereby specifically facilitating FoxO3 deacetylation. We determined that geminin–associated HDAC3 deacetylates FoxO3 to block its transcriptional activity, leading to downregulation of the downstream FoxO3 target Dicer, an RNase that suppresses metastasis. Breast cancer cells depleted of geminin or HDAC3 exhibited poor metastatic potential that was attributed to reduced suppression of the FoxO3-Dicer axis. Moreover, elevated levels of geminin, HDAC3, or both together with decreased FoxO3 acetylation and reduced Dicer expression were detected in aggressive human breast cancer specimens. These results underscore a prominent role for geminin in promoting breast cancer metastasis via the enzyme-substrate–coupling mechanism in HDAC3-FoxO3 complex formation.

Introduction

Acetylation can modulate numerous transcription factors, nuclear regulators, and cytoplasmic proteins that are involved in diverse cellular functions (1, 2). Histone deacetylase (HDAC) enzymes, including members of the zinc-dependent RPD3/HDA1 family and the NAD^+-dependent sirtuin family, are known to reverse acetylation, thereby restoring the positive charge of the lysine residues of the substrate proteins. Based on sequence homology (3) and other phylogenetic analyses, the 18 HDACs in humans can be further grouped into 4 classes. Class I contains HDAC1,-2,-3, and -8. Class IIa members are HDAC4,-5,-7, and -9. Class IIb includes HDAC6 and HDAC10, whereas HDAC11 is known as class IV. The members of the sirtuin family are grouped into class III. It has been shown that class I and class III HDACs are catalytic subunits of multiprotein complexes that can interact with transcription factors to activate or suppress gene transcription, thereby regulating cellular homeostasis and stress responses (4–7).

The forkhead box (FoxO) transcription factors are pivotal regulators in maintaining cellular homeostasis (8, 9). Among the mammalian FoxO family members, FoxO1 and FoxO3 are highly homologous in their protein sequences. These 2 FoxOs are often expressed in the same types of cells and are subjected to phosphorylation and acetylation (10, 11). However, evidence from gene-knockout studies revealed that FoxO1 and FoxO3 proteins have distinct physiological functions. While FoxO1-deficient mice are embryonic lethal due to defects in angiogenesis (12, 13), FoxO3-deficient animals become infertile due to global primordial follicle activation with subsequent oocyte exhaustion (14). It remains unknown which specific modifications result in the functional difference of these 2 family members.

We previously found that FoxO3 has a unique role in regulating G_1/S transition via stabilizing the chromatin licensing and DNA replication factor 1 (CDT1) protein, a binding partner of geminin (15). Geminin is a negative factor involved in DNA replication by blocking CDT1, thereby maintaining chromosomal integrity and preventing aneuploidy (16, 17). Loss of function of geminin was found to specifically induce DNA rereplication, DNA damage, and apoptosis in malignant cancer cells, whereas normal or immortalized cells remain insensitive to geminin ablation (18), raising the possibility that geminin may serve as a potential target for cancer treatment. Emerging evidence also has revealed multiple roles for geminin, through interaction with a number of epigenetic modulators or transcription factors, in cell-fate decision during development (19–23). Interestingly, despite its role in guarding genome integrity, geminin has recently been reported as exhibiting oncogenic activity for elevated geminin expression, which is positively correlated with the aggressive clinical behaviors of various types of human cancers (24, 25). For instance, geminin is frequently overexpressed in breast cancers, and its dysregulation

Conflict of interest: The authors have declared that no conflict of interest exists.
Submitted: August 10, 2016; **Accepted:** February 21, 2017.
Reference information: *J Clin Invest*. 2017;127(6):2159–2175.
https://doi.org/10.1172/JCI90077.

predicts a poor clinical outcome (26, 27). Little is known regarding the molecular mechanism underlying geminin-mediated tumorigenesis and cancer metastasis. Of note, contradictory reports have proposed positive and negative roles for geminin in regulating epithelial-to-mesenchymal transition during development (28, 29).

Given that both geminin and FoxO3 can form protein complexes with CDT1, we analyzed FoxO3 and geminin protein-protein interaction. Geminin directly associated with FoxO3, which in turn blocked its transcriptional activity. Surprisingly, FoxO3 turns on *Dicer*, a member of the RNaseIII superfamily for miRNA biogenesis (30). We further demonstrated that *Dicer* is a downstream target of FoxO3 and mediates FoxO3 metastasis-suppression function. As a binding partner of FoxO3, geminin abrogated the transactivation of *Dicer* by FoxO3 via tethering HDAC3 to deacetylate FoxO3. Our results established a crucial effect of geminin as the enzyme-substrate coupling factor involved in FoxO3-HDAC3 complex formation and provide mechanistic insights into geminin-mediated tumorigenesis and cancer metastasis.

Results

Geminin interacts with FoxO3. We have reported that FoxO3 interacts with CDT1 (15), a key component of the prereplicative complex. Since CDT1 is a binding partner of geminin, we tested to determine whether FoxO3 associated with geminin. Ectopically expressed FLAG-FoxO3 and Myc-geminin bound to each other, as indicated by reciprocal immunoprecipitation experiments (Supplemental Figure 1, A and B; supplemental material available online with this article; https://doi.org/10.1172/JCI90077DS1). The interaction between endogenous FoxO3 and geminin was readily detected using cell lysates from LM2 cells (Figure 1A), which are derived from MDA-MB-231 cells with strong lung metastasis potential (31). Pull-down assays showed a direct physical interaction between FoxO3 and geminin proteins (Supplemental Figure 1C).

To identify the domain of geminin required for FoxO3 interaction, we generated geminin subdomain constructs. The coiled-coil domain (CCD) was sufficient for interaction with FoxO3 (Figure 1B). Geminin–leucine zipper (geminin-LZ), a dimerization-deficient mutant (Supplemental Figure 1D), failed to associate with FoxO3 (Figure 1B), indicating that dimerization might be a prerequisite for geminin associating with FoxO3. To further identify key residues of the CCD required for FoxO3 interaction, we generated a series of geminin CCD mutants, namely E92A, E101A, E104A, E101/104A, E112A, E116A, E123A, E130A, and E137A. These negatively charged glutamic acids have been shown to be critical for geminin-CDT1 and geminin–homeobox A1 (geminin-HoxA1) interaction (32). Among them, GEM^{E130A} (a dimerization-competent mutant) completely abolished geminin-FoxO3 interaction (Figure 1C, and Supplemental Figure 1, D and E). Mapping the region of FoxO3 required for geminin binding revealed a crucial role of the DNA-binding domain (DBD) in protein complex formation (Supplemental Figure 1F). In particular, the aa150–aa160 segment of the DBD mediated its association with geminin (Figure 1, D and E). Since DBD is highly conserved among FoxO family members, we tested to determine whether geminin associated with other FoxO proteins. Purified FoxO1 was found to interact with geminin by glutathione S-transferase (GST) pull-down assay (Supplemental Figure 1G). Further analysis revealed that residues 154–163 of FoxO1 DBD were required for its binding with geminin (Supplemental Figure 1H). However, in LM2 cells, geminin has about a 20-fold greater affinity for FoxO3 than for FoxO1 (Figure 1A), suggesting that geminin preferentially interacts with FoxO3 in vivo.

We reasoned that a second part of FoxO3 outside the DBD interacted with geminin and that this segment may serve as the key determinant of FoxO3-geminin interaction. To identify this second part, serial truncations were made to the N terminus of FoxO3 (Figure 1D). As shown in Figure 1E, residues 1–120 of FoxO3 retained the interacting ability with geminin, while residues 1–100 could not bind geminin, suggesting that FoxO3 100–120 residues interact with geminin. Of note, the amino acid sequences of the FoxO3 100–120 region are not conserved in FoxO1 or FoxO4 (Supplemental Figure 1I). As expected, FoxO1 1–140 failed to associate with geminin (Supplemental Figure 1H). Moreover, 100–120 deletion profoundly abrogated FoxO3-geminin complex formation, whereas a FoxO3 construct lacking residues 150–160 was capable of binding to geminin with an affinity nearly identical to that of WT FoxO3 (Figure 1F). Depletion of both regions completely abolished FoxO3 interaction with geminin (Figure 1F). These results demonstrate that discrimination between the FoxO family members is governed by geminin contacts to residues 100–120 of FoxO3.

FoxO3 regulates Dicer expression and miRNA biosynthesis. When coexpressed with a triple mutant form of FoxO3 in which all three Akt phosphorylation sites are mutated to alanine (T32A/S253A/S315A) (FoxO3-TM), a constitutively active mutant form of FoxO3, geminin profoundly abrogated FoxO3-TM–driven forkhead response element (FHRE)-luciferase reporter (a commonly used luciferase reporter for reflecting the transcriptional activity of FoxOs) activity (Supplemental Figure 2A), suggesting that geminin repressed FoxO3-mediated transcription. We previously characterized the transcriptional profiles of human colon cancer cell line HCT116 cells depleted of FoxO3 by genome-wide RNA sequencing (RNA-seq). *Dicer* gene expression was significantly inhibited in FoxO3-depleted cells (Supplemental Table 1), but activated in geminin-knockdown cells (Supplemental Figure 2B). Further validation in a variety of human cancer cell lines confirmed that *Dicer* gene expression was markedly decreased upon FoxO3 depletion (Figure 2A and Supplemental Figure 2, C–J). We next utilized an inducible FoxO3-TM mutant as described before (33) to verify the regulation of *Dicer* by FoxO3. When HCT116 cells were treated with 4-hydroxytamoxifen (4-OHT), *Dicer* expression was robustly induced only in FoxO3-TM, but not in FoxO3-TMΔDB (a FoxO3-TM form lacking DBD), cells (Supplemental Figure 2, K and L). Of note, silencing FoxO1 or FoxO4 in MDA-MB-231 cells failed to downregulate *Dicer* levels (Supplemental Figure 2, M and N), demonstrating a unique role for FoxO3 in directing *Dicer* expression.

To determine whether *Dicer* is a transcriptional target of FoxO3, we searched the promoter region of the human *Dicer* gene and found one site in the 5′ UTR region that matched the consensus FoxO-binding element (FBE). Luciferase reporter assay showed that the *Dicer-luciferase* reporter only responded to WT FoxO3 or FoxO3-TM, but not FoxO3-TMΔDB. Mutation of the core FBE profoundly attenuated luciferase activity (Figure 2B). ChIP analysis further revealed that endogenous FoxO3 protein only bound to the FBE site (amplicons 2 and 3) on the *Dicer* promoter, but not the

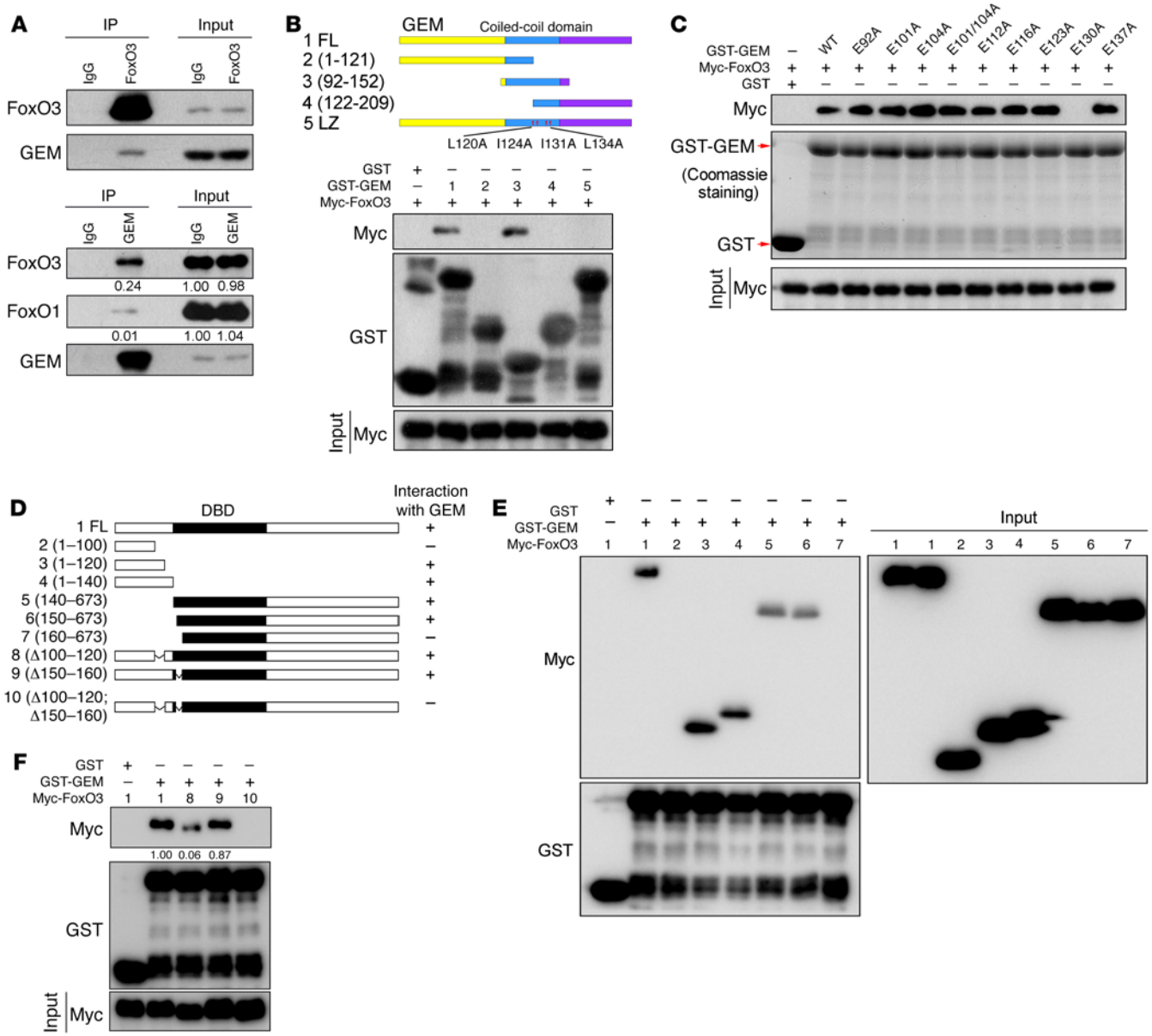

Figure 1. Geminin interacts with FoxO3. (**A**) LM2 cell lysates were subjected to immunoprecipitation with anti-FoxO3, anti-geminin, or control IgG. The immunoprecipitates were then blotted with the indicated antibodies. (**B** and **C**) HEK-293T cells transfected with Myc-FoxO3 were lysed, and lysates were incubated with the indicated GST recombinant proteins. Proteins retained on sepharose were then blotted with the indicated antibodies. (**D**) Schematic diagram of WT and FoxO3 mutants. (**E** and **F**) HEK-293T cells transfected with the indicated constructs were lysed, and lysates were incubated with GST or GST-geminin (GST-GEM) coupled to GSH-sepharose. Proteins retained on sepharose were then blotted with the indicated antibodies.

2 control sites (amplicons 1 and 4), indicating that FoxO3 regulates *Dicer* transcriptionally (Figure 2, C and D). Introducing FoxO3 shRNA completely abrogated the binding of FoxO3 protein to the *Dicer* promoter (Figure 2, C and D), ensuring the specificity of the anti-FoxO3 ChIP signals. Notably, this FBE site is not conserved in the murine *Dicer* promoter. Furthermore, knockdown of FoxO3 in 2 independent murine cell lines had no detectable effect on Dicer expression (Supplemental Figure 2, O and P), suggesting that the transactivation of *Dicer* by FoxO3 is human specific.

Dicer is a key component of the miRNA-processing machinery. We next examined the impact of FoxO3 knockdown on miRNA biosynthesis by array analysis of miRNA expression profiles. Strikingly, mature miRNAs were globally downregulated in MDA-MB-231 cells depleted of FoxO3 (Figure 2E and Supplemental Table 2). When we measured 3 miRNAs that have a recognized role in metastasis, namely miR-206, miR-335, and miR-429, we found their mature miRNAs, but not the primary miRNAs, were significantly downregulated (Figure 2, F and G). Moreover, Dicer reconstitution significantly restored the expression levels of these miRNAs in FoxO3-depleted cells (Figure 2, G and H), indicating that Dicer is the major downstream effector mediating the role of FoxO3 in miRNA biogenesis.

In *Drosophila,* Dicer-1 (Dcr1) is involved in miRNA biogenesis and Dcr2 regulates siRNA biogenesis (34, 35). A recent report

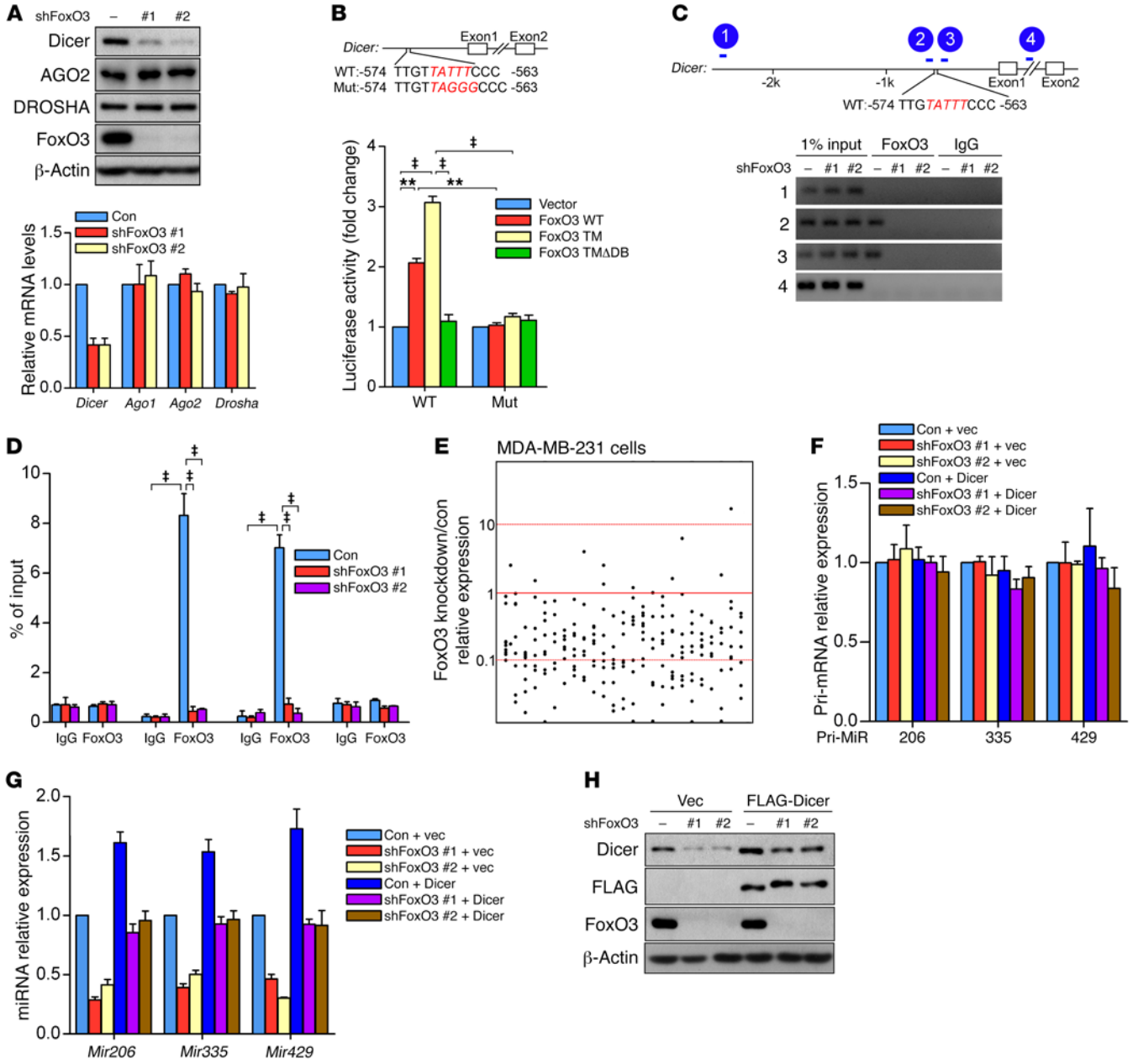

Figure 2. FoxO3 regulates Dicer expression and miRNA biosynthesis. (**A**) LM2 cells were infected with lentivirus encoding FoxO3 shRNAs. Cell lysates and RNA were extracted and subjected to Western blotting (upper panel) or qRT-PCR (lower panel), respectively. Results are shown as mean ± SD. *n* = 3 independent experiments. (**B**) Luciferase assay of HEK-293T cells cotransfected with the *Dicer* promoter luciferase reporter and the indicated FoxO3 constructs. Upper panel: schematic of the *Dicer* promoter, showing the sequence of the putative FBEs in the human *Dicer* promoter region and the substitution mutations introduced into this FBE sequence. Lower panel: luciferase reporter activity results are depicted as bar graph with mean ± SD. *n* = 3 independent experiments. ‡$P < 0.001$; **$P < 0.01$, 2-way ANOVA with Bonferroni's post hoc test. (**C**) ChIP assay in LM2 cells. Diagram of the *Dicer* promoter region with the amplicons used for PCR analysis (upper panel). ChIP analysis for the presence of FoxO3 at the *Dicer* promoter in LM2 cells with or without FoxO3 depletion (lower panel). (**D**) Data from **C** are depicted as bar graph with mean ± SD. *n* = 3 independent experiments. ‡$P < 0.001$, 2-way ANOVA with Bonferroni's post hoc test. Con, control. (**E**) Dots show the ratio of miRNA expression levels in MDA-MB-231 cells depleted of FoxO3. (**F** and **G**) LM2 cells were infected with lentivirus encoding the indicated shRNAs. RNA was extracted and subjected to qRT-PCR. Results are shown as mean ± SD. *n* = 3 independent experiments. (**H**) LM2 cells stably expressing FLAG-Dicer and the indicated shRNAs were subjected to Western blotting.

revealed the regulation of Dcr2 by *Drosophila* FoxO (dFoxO) in flies (36). In humans, there is only 1 Dicer, which is involved in both miRNA and siRNA processing. Unlike in *Drosophila*, in human cells, FoxO3 solely transactivated *Dicer* without showing any effect on AGO1 and/or AGO2, 2 components involved in miRNA processing and function (Figure 2A and Supplemental Figure 2, C–J). In addition, FoxO3 silencing failed to change levels of Drosha (Figure 2A and Supplemental Figure 2, C–J), another RNase III enzyme in miRNA biogenesis. These results indicate that FoxO3 in mammals directs miRNA production in large part through transactivating

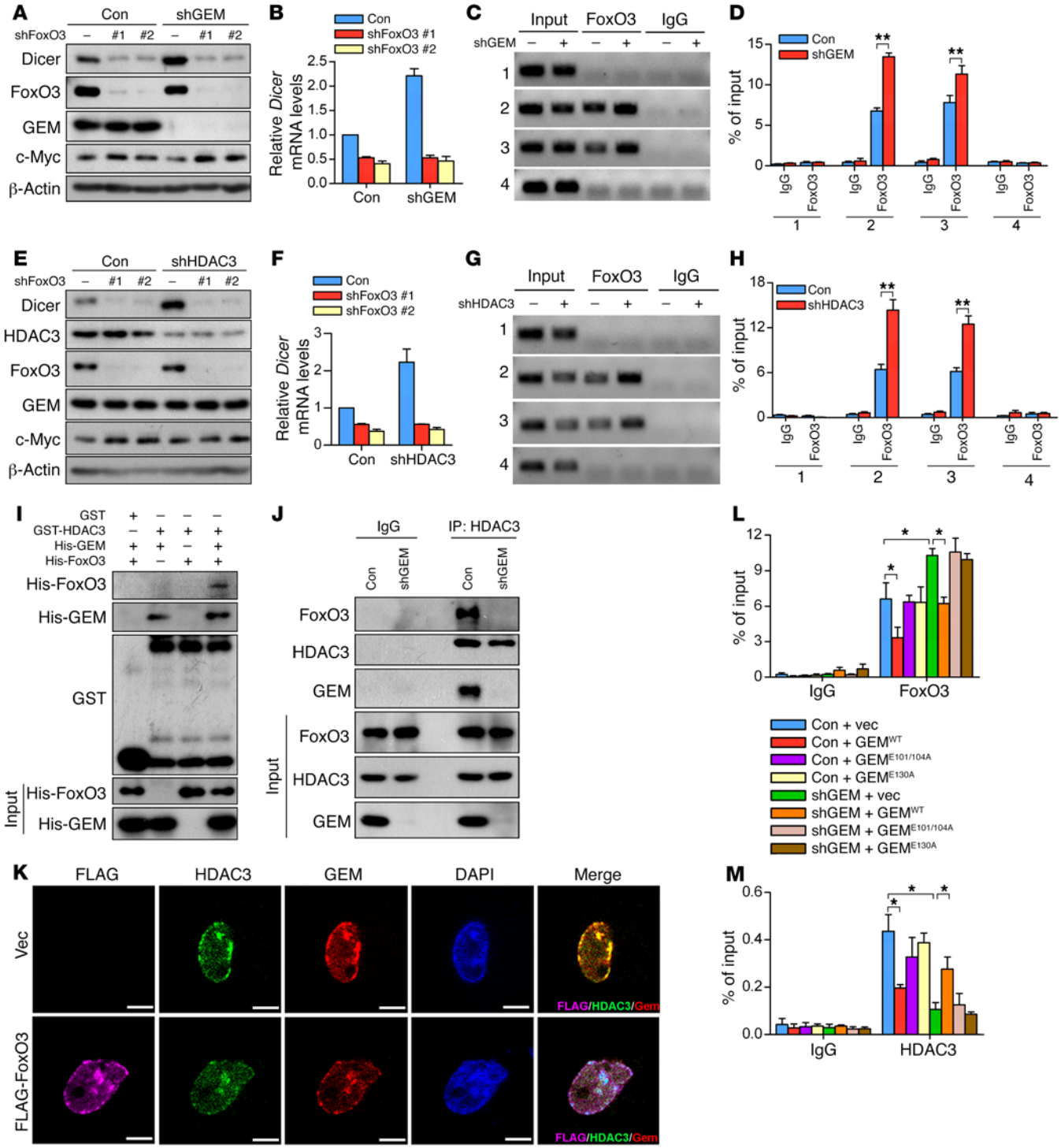

Figure 3. Geminin suppresses Dicer expression via coupling HDAC3 to FoxO3. (**A** and **B**) Whole cell lysates prepared from LM2 cells infected with lentivirus encoding the indicated shRNAs were subjected to Western blotting analysis with indicated antibodies (**A**) and qRT-PCR analysis of *Dicer* mRNA levels (**B**). (**C** and **D**) Anti-FoxO3 or control IgG was used for ChIP assay to analyze the occupancy of FoxO3 on the *Dicer* promoter in LM2 cells with control versus geminin depletion (**C**). Quantification results are shown (**D**). $n = 3$ independent experiments. $^{**}P < 0.01$, 2-tailed Student's t test. (**E** and **F**) LM2 cells infected with lentivirus encoding the indicated shRNAs were subjected to Western blotting analysis with the indicated antibodies (**E**). qRT-PCR analysis of *Dicer* mRNA levels are shown (**F**). (**G** and **H**) ChIP assay to analyze the occupancy of FoxO3 on *Dicer* promoter in control versus HDAC3-depleted LM2 cells (**G**). Quantification results are shown (**H**). $n = 3$ independent experiments. $^{**}P < 0.01$, 2-tailed Student's t test. (**I**) Purified geminin and/or FoxO3 recombinant proteins were incubated with GST or GST-HDAC3. Proteins retained on sepharose were then blotted with the indicated antibodies. (**J**) Lysates from LM2 cells expressing geminin shRNA (shGEM) were subjected to immunoprecipitation with HDAC3 antibody followed by immunoblotting with anti-FoxO3, anti-HDAC3, and anti-geminin. (**K**) LM2 cells were infected with lentivirus-encoding vector or FLAG-FoxO3 for 72 hours. Cells were then fixed and stained with the indicated antibodies. Colocalization of the indicated proteins was visualized by confocal microscope. Scale bars: 10 μm. (**L** and **M**) ChIP to analyze the occupancy of FoxO3 (**L**) or HDAC3 (**M**) on *Dicer* promoter in geminin-depleted LM2 cells reconstituted with the indicated geminin constructs. $n = 3$ independent experiments. $^{*}P < 0.05$, 2-way ANOVA with Bonferroni's post hoc test.

Dicer expression. Thus, dFoxO and human FoxO3 (hFoxO3) control miRNA/siRNA biogenesis via different mechanisms.

Geminin suppresses Dicer expression via coupling of HDAC3 to FoxO3. The upregulation of Dicer in geminin-deficient HCT116 cells prompted us to investigate whether there is a negative correlation between these 2 molecules. The protein levels of Dicer and geminin were inversely correlated in nonmetastatic breast cancer cell line MCF-7 as well as highly metastatic cell lines MDA–MB-231 and LM2 (Supplemental Figure 3A). Moreover, MCF-7 cells exhibited much higher expression levels of Dicer and FoxO3 compared with the other 2 breast cancer cell lines. In contrast, FoxO1 levels showed no difference among all these cell lines (Supplemental Figure 3A). When ectopically expressed in LM2 cells, GEM^{WT} but not GEM^{E130A} profoundly blunted basal Dicer expression at both protein and mRNA levels (Supplemental Figure 3, B and C). Conversely, geminin deficiency led to Dicer upregulation in LM2 cells (Figure 3, A and B). Given that geminin formed a complex with FoxO3, we asked whether geminin influenced Dicer levels in a FoxO3-dependent manner. To test this, we depleted FoxO3 and geminin individually or together. Dicer accumulation in geminin-depleted cells was completely abrogated upon FoxO3 ablation (Figure 3, A and B), supporting the conclusion that geminin modulated Dicer expression via FoxO3. Consistently, GEM^{WT} but not GEM^{E130A} profoundly inhibited *Dicer–luciferase* reporter activity driven by FoxO3-TM (Supplemental Figure 3D). ChIP assay using geminin antibody confirmed the occupancy of geminin at the *Dicer* promoter (Supplemental Figure 3E). Sequential ChIP experiments (FoxO3 ChIP followed by geminin ChIP) showed that endogenous FoxO3 and geminin cooccupied the *Dicer* promoter region (Supplemental Figure 3F). Moreover, an increasing enrichment of FoxO3 at the *Dicer* promoter was observed when geminin was silenced (Figure 3, C and D). These results indicate that geminin exerts a negative effect on FoxO3-dependent transactivation of *Dicer* via interfering with its binding to the *Dicer* promoter.

The interaction of geminin with the DBD of FoxO3 raised the possibility that the subsequent inhibition of FoxO3 may be attributed to a direct "wedge" effect of geminin in blocking FoxO3 DNA association. Alternatively, geminin may influence the posttranslational modification of FoxO3, which in turn impairs FoxO3 DNA–binding affinity. We next set out to distinguish these two possibilities. Previous studies have shown that geminin recruited HDAC3 to regulate chromatin acetylation and gene expression (37). HDAC3 is known to deacetylate FoxO members to modulate their transcriptional activities (6, 38). To determine whether HDAC3 has any role in geminin-dependent suppression of FoxO3, we first investigated whether HDAC3 influenced the FoxO3-Dicer axis. Dicer accumulated in LM2 cells when HDAC3 was depleted, but not in LM2 cells further depleted of FoxO3 (Figure 3, E and F). ChIP analysis revealed the association of HDAC3 with the *Dicer* promoter (Supplemental Figure 3G). Moreover, ectopic HDAC3 profoundly abolished FoxO3-TM–driven *Dicer-luciferase* reporter activity (Supplemental Figure 3H), and HDAC3 knockdown significantly increased FoxO3 occupancy at the *Dicer* promoter (Figure 3, G and H), all highlighting a suppressive role of HDAC3 in FoxO3-dependent transactivation of *Dicer*. Previous studies reported that HDAC3-mediated FoxO3 deacetylation regulated miR-34c for expression, leading to c-Myc upregulation in glioblastoma cells (38). Consistently, we found c-Myc protein levels were elevated upon FoxO3 knockdown (Figure 3, A and E). However, miR-34c levels remained unchanged in FoxO3-depleted LM2 cells (Supplemental Figure 3I). Furthermore, silencing geminin or HDAC3 barely affected c-Myc expression (Figure 3, A and E), suggesting the FoxO3–miR-34c axis might be context dependent.

HDAC3 knockdown phenocopied the effect of geminin depletion on FoxO3-mediated transactivation of *Dicer*, raising the possibility that geminin may influence the FoxO3-Dicer axis through HDAC3. We speculated that geminin, HDAC3, and FoxO3 formed a multiprotein complex. In HEK-293T cells, ectopically expressed geminin and HDAC3 interacted with each other (Supplemental Figure 3J). A direct interaction between these two proteins was confirmed by using purified HDAC and geminin proteins for affinity binding analysis (Supplemental Figure 3K). While aa181–aa313 of HDAC3 was required for geminin binding (Supplemental Figure 3L), geminin with E101A and E104A double mutation (denoted as $GEM^{E101/104A}$) disrupted its association with HDAC3 (Supplemental Figure 3, M–O). Given that HDAC3 does not directly associate with FoxO members (6), we hypothesized that geminin may serve as a molecular scaffold for the interaction of FoxO3 and HDAC3. GST pull-down assays confirmed that HDAC3 bound to FoxO3 only when geminin was present (Figure 3I). Conversely, HDAC3 failed to interact with FoxO3 in the absence of geminin (Figure 3J), supporting the notion that HDAC3 associates with FoxO3 through geminin. The colocalization of ectopic FoxO3 with endogenous geminin and HDAC3 proteins was visualized in the nucleus of LM2 cells (Figure 3K). We next determined whether geminin and HDAC3 are mutually dependent on FoxO3-driven Dicer expression. GEM^{WT} but not $GEM^{E101/104A}$ inhibited FoxO3-TM–driven *Dicer*-promoter luciferase reporter activity (Supplemental Figure 3P) and suppressed Dicer expression in LM2 cells (Supplemental Figure 3Q). ChIP results revealed a significantly reduced capacity of HDAC3 to bind to the *Dicer* promoter in the absence of geminin (Supplemental Figure 3R). These results indicate that geminin is critical for the binding of HDAC3 to the *Dicer* promoter and that HDAC3 in turn is indispensable for geminin-mediated suppression of FoxO3 transcriptional activity.

We next determined whether geminin inhibits FoxO3 via its physical interaction with FoxO3 and HDAC3. To this end, we reconstituted geminin-depleted cells with GEM^{WT} or the binding-defective geminin mutants GEM^{E130A} and $GEM^{E101/104A}$. FoxO3 enrichment at the *Dicer* promoter was blocked only by GEM^{WT}, not the geminin mutants (Figure 3L). Likewise, only GEM^{WT} restored the recruitment of HDAC3 to the *Dicer* promoter in geminin-deficient cells (Figure 3M). We noticed that GEM^{WT} overexpression profoundly abrogated the association of FoxO3 or HDAC3 with the *Dicer* promoter (Figure 3, L and M), which was likely attributed to the attenuated binding capacity of FoxO3 to the DNA. Since $GEM^{E101/104A}$ is capable of FoxO3 binding, these results demonstrated that geminin suppressed FoxO3 DNA–binding activity mainly through tethering HDAC3 to FoxO3, rather than by sterically hindering the access of FoxO3 to DNA.

Geminin inhibits FoxO3 via recruiting HDAC3 to deacetylate FoxO3. Given that HDAC3 or geminin depletion led to an enhanced FoxO3-*Dicer* promoter interaction and a subsequent upregulation of Dicer, it is plausible that the suppressive effect of HDAC3 or gem-

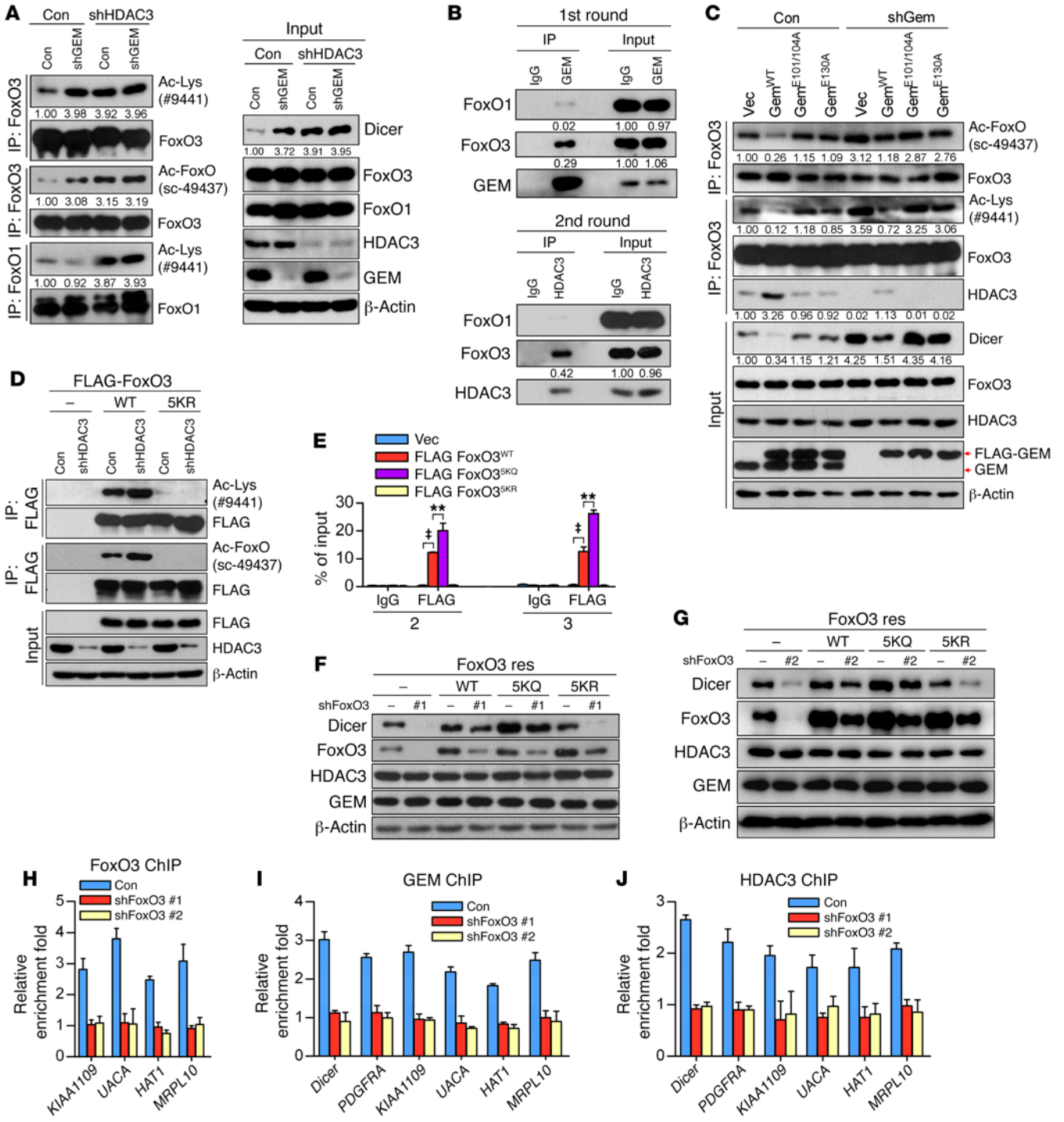

Figure 4. Geminin inhibits FoxO3 via recruitment of HDAC3 to deacetylate FoxO3. (**A**) LM2 cells infected with the indicated lentiviral constructs were lysed and subjected to immunoprecipitation with FoxO3 or FoxO1 antibodies. The immunoprecipitates were then blotted with anti–Ac-Lys, anti-FoxO3, anti–Ac-FoxO, and anti-FoxO1 (left panel). Total lysates were analyzed by Western blotting (right panel). (**B**) Two-step coimmunoprecipitation identifies a FoxO3-geminin-HDAC3 complex. LM2 cell lysates were first precipitated with anti-geminin and eluted with the polypeptide against which the geminin antibody was raised. Elutes were then immunoprecipitated with anti-HDAC3 or control IgG. Protein samples from each step were analyzed by immunoblotting with the indicated antibodies. (**C**) Geminin-depleted LM2 cells were reconstituted with the indicated geminin constructs. Cell lysates were subjected to immunoprecipitation with FoxO3 antibody. The immunoprecipitates were then blotted with the indicated antibodies. (**D**) FoxO3-depleted LM2 cells infected with lentivirus encoding the indicated shRNAs were lysed, and lysates were subjected to immunoprecipitation with anti-FLAG. The immunoprecipitates were then blotted with the indicated antibodies. (**E**) ChIP to analyze the occupancy of FLAG-FoxO3 (WT, 5KQ, 5KR) on *Dicer* promoter in LM2 cells. $n = 3$ independent experiments. $^{‡}P < 0.001$; $^{**}P < 0.01$, 2-way ANOVA with Bonferroni's post hoc test. Vec, vector. (**F** and **G**) LM2 cells were infected with the indicated lentiviral constructs. Cell lysates were extracted and subjected to Western blotting. (**H**–**J**) ChIP analysis for the presence of FoxO3 (**H**), GEM (**I**), or HDAC3 (**J**) at the *Dicer* promoter in LM2 cells with or without FoxO3 depletion.

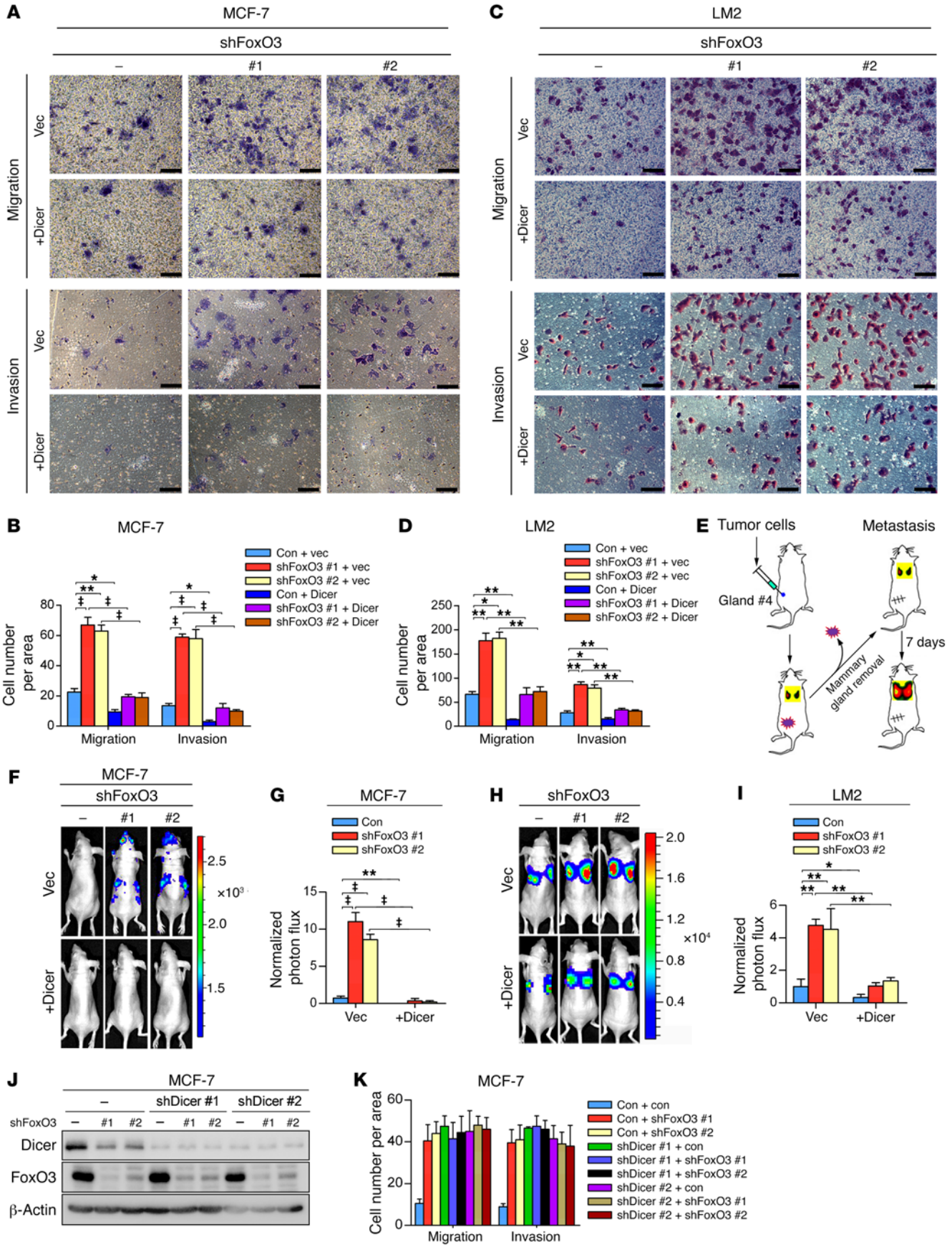
A
MCF-7
shFoxO3
–
#1
#2
Migration
Invasion
Vec
+Dicer
C
LM2
B
MCF-7
Con + vec
shFoxO3 #1 + vec
shFoxO3 #2 + vec
Con + Dicer
shFoxO3 #1 + Dicer
shFoxO3 #2 + Dicer
Cell number per area
Migration
Invasion
D
LM2
E
Tumor cells
Metastasis
Gland #4
7 days
Mammary gland removal
F
MCF-7
shFoxO3
×10³
G
MCF-7
Con
shFoxO3 #1
shFoxO3 #2
Normalized photon flux
Vec
+Dicer
H
shFoxO3
×10⁴
I
LM2
J
MCF-7
shDicer #1
shDicer #2
Dicer
FoxO3
β-Actin
K
MCF-7
Con + con
Con + shFoxO3 #1
Con + shFoxO3 #2
shDicer #1 + con
shDicer #1 + shFoxO3 #1
shDicer #1 + shFoxO3 #2
shDicer #2 + con
shDicer #2 + shFoxO3 #1
shDicer #2 + shFoxO3 #2
Cell number per area

Figure 5. FoxO3 regulates metastasis through Dicer. (**A**–**D**) MCF-7 cells (**A** and **B**) or LM2 cells (**C** and **D**) infected with the indicated lentiviral constructs were subjected to Transwell migration and invasion assays. Results are shown as mean ± SD. n = 3 independent experiments. Scale bars: 50 μm. ‡P < 0.001; **P < 0.01; *P < 0.05, 2-way ANOVA with Bonferroni's post hoc test. (**E**) Experimental design for in vivo metastasis analysis using orthotropic injection. (**F**–**I**) Luciferase-labeled MCF-7 cells (**F** and **G**) or LM2 cells (**H** and **I**) infected with lentivirus encoding the indicated shRNAs were injected into the mammary fat pads of nude mice. Representative bioluminescence imaging (BLI) images of mice with spontaneous lung metastasis (**F** and **H**) and quantification of the bioluminescence signal (**G** and **I**) are shown. Results represent mean ± SD; n = 8 mice per group. ‡P < 0.001; **P < 0.01; *P < 0.05, 2-way ANOVA with Bonferroni's post hoc test. (**J**) MCF-7 cells were infected with lentivirus encoding FoxO3 and/or Dicer shRNAs. Cell lysates were extracted and subjected to Western blotting. (**K**) Cells from **J** were subjected to Transwell migration and invasion assays. Results are shown as mean ± SD. n = 3 independent experiments.

inin on FoxO3 transcriptional activity may involve deacetylation of FoxO3. This hypothesis prompted us to analyze FoxO3 acetylation in cells with geminin or HDAC3 ablation. Immunoprecipitated FoxO3 proteins from LM2 cells were analyzed with either pan-acetyl lysine antibody (catalog 9441; Cell Signaling Technology) or acetyl-FKHR antibody (sc-49437; Santa Cruz Biotechnology Inc.). The acetyl-FKHR antibody, originally developed for detection of FoxO1 acetylation on K259, K262, and K271 residues, has been found to recognize acetyl-FoxO3 as well (6), apparently due to the fact that these lysine residues are highly conserved in these FoxO family members. As expected, these antibodies detected identical patterns of acetyl-FoxO members, ensuring the specificity of acetyl-FoxO3 signals. Although HDAC3 silencing in LM2 cells significantly increased acetylation levels of both FoxO1 and FoxO3 (Figure 4A and Supplemental Figure 4A), geminin depletion induced only acetyl-FoxO3, not acetyl-FoxO1 (Figure 4A and Supplemental Figure 4A), which may be due to a binding preference of geminin for FoxO3 over FoxO1. This was further supported by sequential IP results showing that only the FoxO3-geminin-HDAC3 complex was readily detectable in vivo (Figure 4B). We noticed that in the absence of HDAC3, geminin silencing failed to increase FoxO3 acetylation intensity as well as Dicer accumulation (Figure 4A and Supplemental Figure 4A). Furthermore, ectopic GEM^{WT}, but not GEM^{E130A} or $GEM^{E101/104A}$, was able to block acetyl-FoxO3 accumulation in geminin-depleted cells (Figure 4C and Supplemental Figure 4B). These results demonstrate that geminin directs HDAC3 specifically to deacetylate FoxO3.

FoxO3 was specifically acetylated at multiple lysine residues, including Lys-242, Lys-259, Lys-262, Lys-271, and Lys-290 (7, 38). To determine whether acetylation facilitated FoxO3 DNA-binding activity, we reconstituted FoxO3-depleted cells with the following shRNA-resistant FoxO3 mutants: acetylation-mimicking KQ mutant ($FoxO3^{5KQ}$) and acetylation-resistant KR mutant ($FoxO3^{5KR}$). As shown in Figure 4D and Supplemental Figure 4C, 5KR mutant was no longer acetylated. ChIP assay revealed that the 5KQ mutant exhibited enhanced binding activity to the *Dicer* promoter, whereas the 5KR mutant showed no binding activity at all (Figure 4E). In line with this, only $FoxO3^{WT}$ and $FoxO3^{5KQ}$ reconstitution restored Dicer expression in FoxO3-depleted cells, whereas $FoxO3^{5KR}$ failed to rescue diminished Dicer expression upon FoxO3 silencing (Figure 4, F and G, and Supplemental Figure 4D).

To investigate whether suppression of FoxO3-mediated gene transcription by geminin is broadly applicable, we searched for additional FoxO3 targets that can be regulated by the geminin/HDAC3 axis. We performed RNA-seq experiments and obtained 27 candidate genes that were coregulated by the geminin-FoxO3 interplay (Supplemental Table 3). Further validation by quantitative real-time PCR (qRT-PCR) revealed that 5 genes, *PDGFRA*, *KIAA1109*, *UACA*, *MRPL10*, and *HAT1*, were repressed by geminin or HDAC3 in a FoxO3-dependent manner (Supplemental Figure 4E). Our previous study showed that *PDGFRA* is a common target of the FoxO family (33). ChIP analysis confirmed that the other 4 genes were FoxO3 downstream targets as well (Figure 4H). Importantly, similarly to $FoxO3^{WT}$ reconstitution, adding back $FoxO3^{5KQ}$ restored expression levels of these genes in FoxO3-depleted cells (Supplemental Figure 4D), suggesting that FoxO3 acetylation positively regulates its transcriptional activity. Further ChIP analysis revealed that promoter occupancy by geminin or HDAC3 with these genes was FoxO3 dependent (Figure 4, I and J). Together, these data indicate that geminin facilitates the deacetylation of FoxO3 by recruiting HDAC3, thereby suppressing the transcriptional activity of FoxO3.

High levels of geminin have been proposed as facilitating hyperacetylation of histones, therefore increasing chromatin accessibility when regulating neural gene expression in mouse embryonic stem cells (39). This prompted us to investigate whether the action of geminin on FoxO3-mediated transcription may also involve a direct modification of histones at the FoxO3 target promoters. To test this hypothesis, we performed the following experiments. We first assessed whether different geminin dosages influence the expression of pan-acetyl-histone H3 (H3ac), H3 acetylated at lysine 9 (H3K9ac), and pan-acetyl-H4 (H4ac) in breast cancers. Unlike in previous findings, we failed to detect any alterations of these proteins in cells expressing ectopic geminin or bearing geminin silencing (Supplemental Figure 4F). We next examined histone modifications on FoxO3 target promoters upon geminin depletion. As shown in Supplemental Figure 4, G–I, ChIP combined with qRT-PCR revealed that geminin knockdown had no effects on acetylation levels of H4, H3, or H3K9 at the indicated promoters. The levels of trimethylated lysine 27 of H3 (H3K27me3) also remained unchanged (Supplemental Figure 4J). These results suggest that suppression of FoxO3-directed transcription by geminin does not involve the indicated histone modifications as previously reported (39).

FoxO3 regulates metastasis through Dicer. Recent studies have demonstrated a pivotal role of Dicer in suppressing tumor metastasis (40). Our observations that *Dicer* is a target gene of FoxO3 prompted us to examine whether FoxO3 controls tumor metastasis via transactivating *Dicer*. To this end, we depleted FoxO3 in breast cancer cells with different metastatic potential. FoxO3 silencing profoundly enhanced the migration and invasion ability in both nonmetastatic (MCF-7) (Figure 5, A and B) and highly metastatic (MDA–MB-231 and LM2) cells (Supplemental Figure 5, A and B and Figure 5, C and D). To assess whether FoxO3 controls metastasis in vivo, we injected FoxO3-depleted cells stably expressing firefly luciferase into the fat pads of immunodeficient nude mice. Metastasis was measured by quantitative bioluminescence imaging. FoxO3-depleted MCF-7 cells displayed significantly, albeit mod-

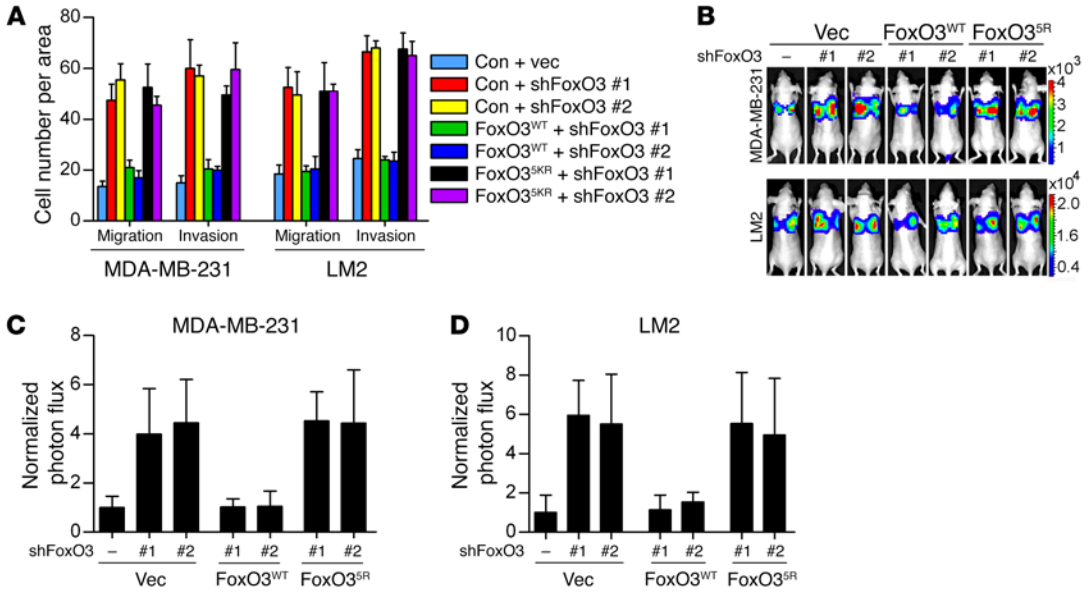

Figure 6. Acetylation of FoxO3 is crucial for suppressing metastasis. (**A**) FoxO3-depleted MDA–MB-231 or LM2 cells reconstituted with FoxO3^{WT} or FoxO3^{5KR} were subjected to Transwell migration and invasion assays. Results are shown as mean ± SD. *n* = 3 independent experiments. (**B**–**D**) Luciferase-labeled MDA–MB-231 or LM2 cells from **A** were injected into the mammary fat pads of nude mice. Representative BLI images of mice with spontaneous lung metastasis (**B**) and quantification of the bioluminescence signal (**C** and **D**) are shown. Results represent mean ± SD; *n* = 6 mice per group.

estly enhanced, metastatic ability 12 weeks after injection (Figure 5, E–G). Likewise, FoxO3 deficiency enabled a more aggressive metastatic phenotype in nude mice injected with MDA–MB-231 or LM2 cells around 6 weeks after injection (Figure 5, H and I, and Supplemental Figure 5, C and D). To elucidate whether FoxO3 controlled metastasis via Dicer, we ectopically expressed Dicer and found that it significantly blunted the metastatic capacity of FoxO3-deficient cells (Figure 5, A–I, and Supplemental Figure 5, A and B). We next assessed the metastasis capacity of cells bearing either individual or compound depletion of FoxO3 and Dicer. As shown in Figure 5, J and K, and Supplemental Figure 5, E–G, knockdown Dicer or FoxO3 alone resulted in significantly enhanced migration and invasion potential. Intriguingly, FoxO3 depletion failed to further enhance metastatic behaviors in Dicer-deficient cells. Collectively, these results indicate that FoxO3 suppresses breast cancer metastasis mainly via Dicer. To rule out any potential shRNA off-target effects and to further confirm that FoxO3^{5KR} mutant indeed resembled loss of function of FoxO3, we performed rescue experiments in FoxO3-depleted cells by adding back shRNA-resistant forms of either FoxO3^{WT} or FoxO3^{5KR}. Only WT shRNA-resistant FoxO3 (FoxO3-Res) significantly repressed metastatic potential both in vitro and in vivo (Figure 6, A–D), whereas FoxO3^{5KR} was incompetent for metastasis suppression. These results suggest that FoxO3 plays a critical role in restraining metastasis and that its acetylation is indispensable for this activity.

When we monitored cell proliferation upon FoxO3 knockdown, we noticed that FoxO3 deficiency failed to alter cell proliferation rates in metastatic breast cancer cells (Supplemental Figure 5, H–J). Previously, we reported that depletion of FoxO3 in MCF-7 cells led to impaired G_1/S transition due to its failure to stabilize CDT1 (15). However, in MDA–MB-231 and LM2 cells, FoxO3 silencing had no detectable effect on the protein levels of CDT1 and geminin (Supplemental Figure 5K). We reasoned that highly metastatic and nonmetastatic breast cancer cells expressed different levels of FoxO3 (Supplemental Figure 5K and Supplemental Figure 3A). In particular, the greatly reduced FoxO3 in metastatic cells was not sufficient to regulate CDT1 protein stability.

DNA replication and gene transcription are two closely linked DNA-templated processes. Geminin is known to play pivotal roles in both processes. To ascertain whether these functions of geminin are interconnected, we first explored whether suppression of FoxO3-dependent gene transcription by geminin contributes to its negative role in DNA rereplication. In agreement with previous studies (41), FACS analysis revealed that a substantial proportion of geminin-deficient HCT116 cells were aneuploidy, which can be rescued by codepletion of CDT1. However, cosilencing of FoxO3 failed to reverse aneuploidy (Supplemental Figure 6, A and B), suggesting that FoxO3 is dispensable for geminin-dependent repression of DNA replication. Similar results were obtained in MCF-7, MDA–MB-231, and LM2 cells (Supplemental Figure 6, C–E). We next determined whether the role of geminin as a DNA replication inhibitor is involved in repressing the FoxO3-Dicer axis and, hence, tumor metastasis. To test this, we depleted CDT1 in geminin-deficient cells, allowing the blockage of the increased aneuploidy, and then examined whether loss of CDT1 can influence the reduced metastatic capacity upon geminin silencing. Disruption of CDT1 in LM2 cells failed to alter Dicer expression and showed no influence on the migration and invasion ability of geminin-depleted cells (Supplemental Figure 6, F–H), suggesting that the regulation of FoxO3-Dicer metastasis by geminin is independent of its suppressive role in DNA replication.

Geminin/HDAC3 complex regulates metastasis through the FoxO3-Dicer axis. Given the ability of geminin to inhibit FoxO3-dependent transactivation of *Dicer* via HDAC3, we asked wheth-

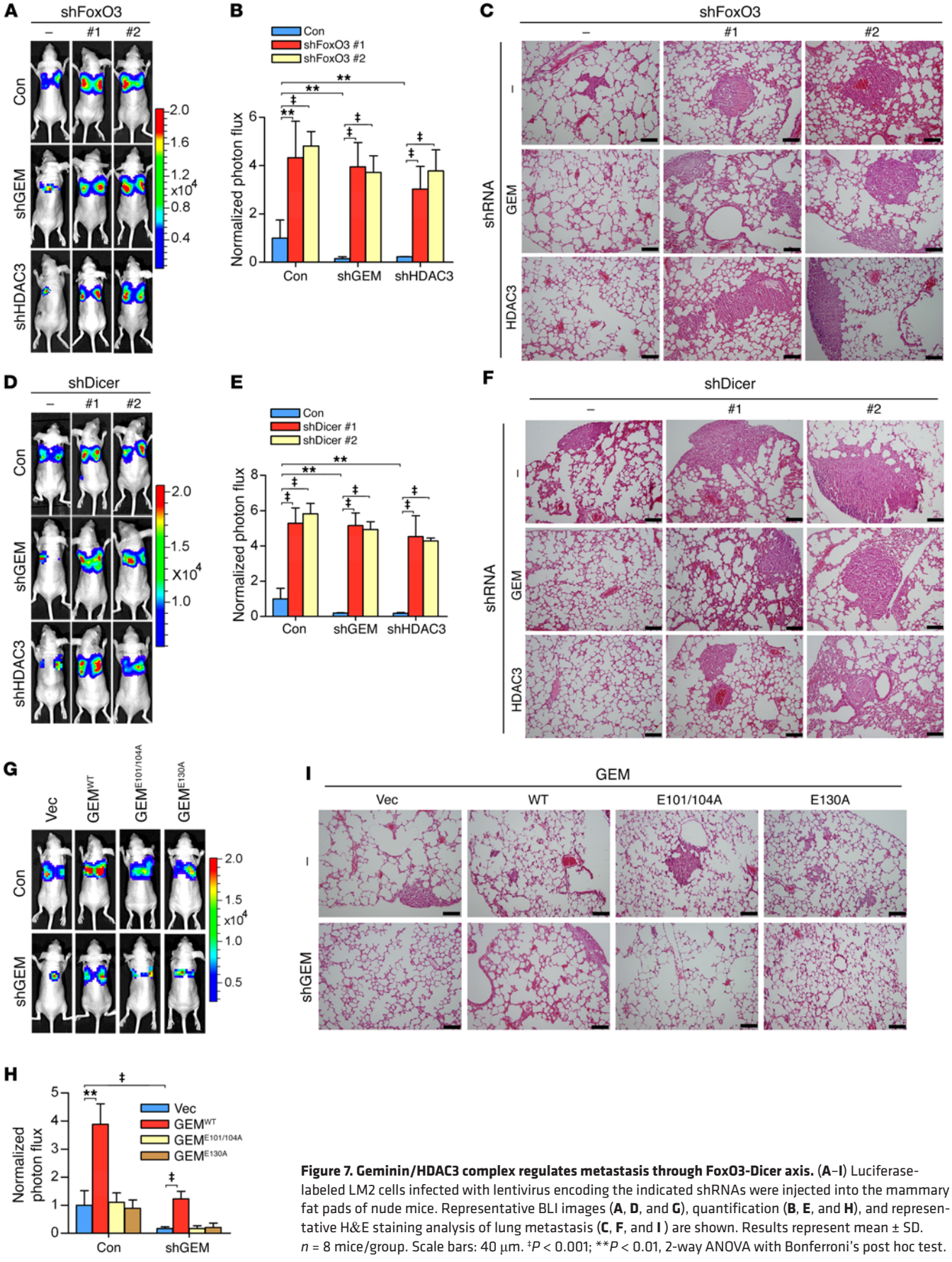

Figure 7. Geminin/HDAC3 complex regulates metastasis through FoxO3-Dicer axis. (**A**–**I**) Luciferase-labeled LM2 cells infected with lentivirus encoding the indicated shRNAs were injected into the mammary fat pads of nude mice. Representative BLI images (**A**, **D**, and **G**), quantification (**B**, **E**, and **H**), and representative H&E staining analysis of lung metastasis (**C**, **F**, and **I**) are shown. Results represent mean ± SD. n = 8 mice/group. Scale bars: 40 μm. ‡$P < 0.001$; **$P < 0.01$, 2-way ANOVA with Bonferroni's post hoc test.

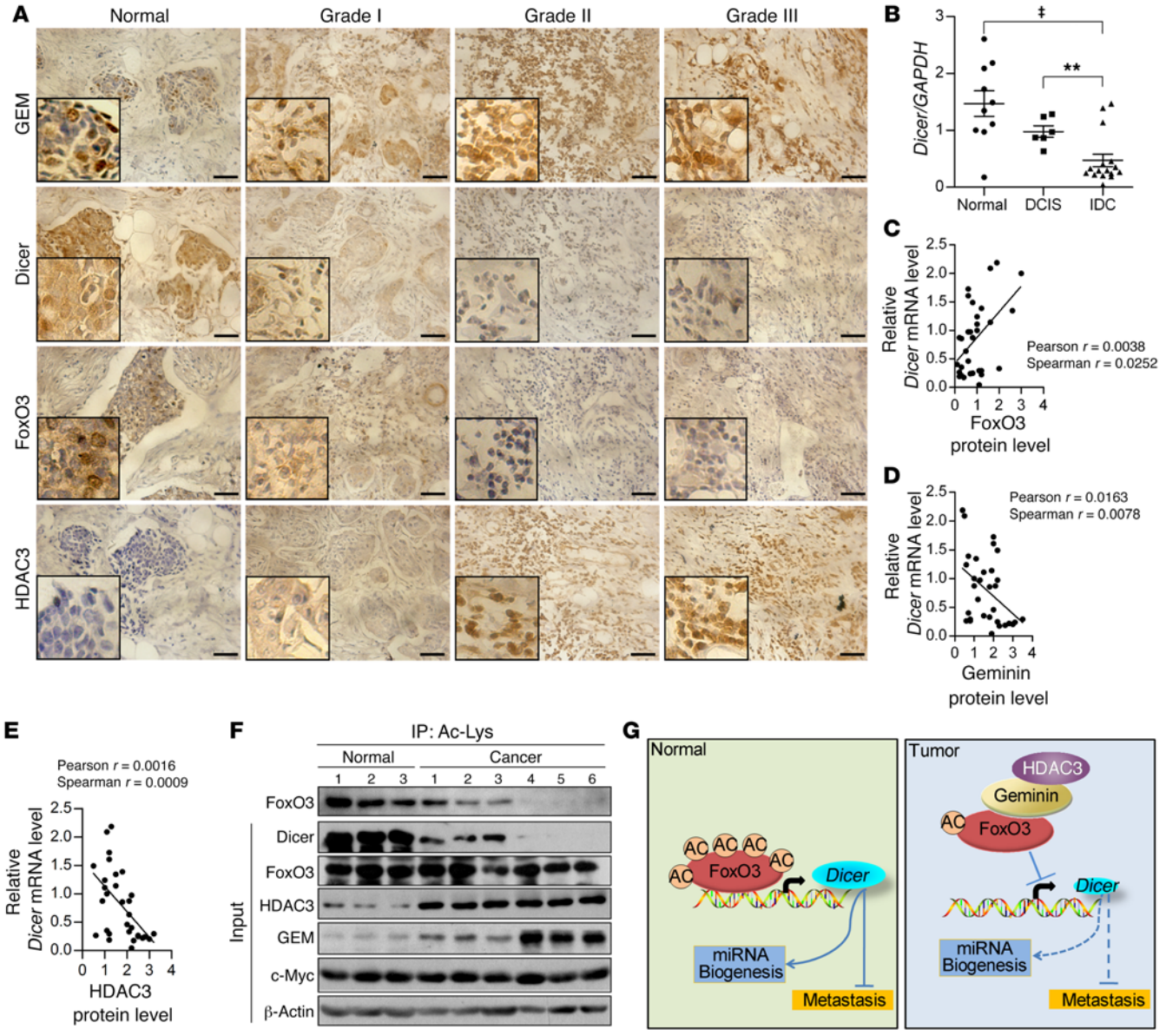

Figure 8. Negative correlation between geminin/HDAC3 and acetyl–FoxO3-Dicer in clinical breast carcinoma samples. (**A**) Immunohistochemical staining of geminin, Dicer, FoxO3, and HDAC3 in normal breast tissues and breast carcinomas (histological grades I, II, and III). Scale bars: 20 μm. (**B**) *Dicer* mRNA levels were analyzed in fresh-frozen tissue samples of normal breast (n = 10), DCIS (n = 6), and IDC (n = 16). $^{**}P < 0.01$; $^{‡}P < 0.001$, 2-tailed unpaired t test. (**C**–**E**) The correlation analysis between FoxO3 (**C**), geminin (**D**), and HDAC3 (**E**) protein and *Dicer* mRNA levels. Correlation coefficient was calculated by Pearson and Spearman correlation analysis. (**F**) IP of normal and IDC samples with anti–Ac-Lys was followed by Western blotting using indicated antibodies. (**G**) Proposed model for geminin/HDAC3-FoxO3-Dicer in breast cancer metastasis regulation.

er this activity underlies the oncogenic properties of geminin, particularly in controlling cancer metastasis. We hypothesized that geminin/HDAC3 should promote metastasis via inhibiting FoxO3-Dicer signaling. As shown in Supplemental Figure 7A and Figure 7, A–C, depletion of either geminin or HDAC3 in LM2 cells led to profoundly decreased migration/invasion potential and the in vivo metastatic capacity of LM2 cells that were apparently not attributed to cell proliferation rates (Supplemental Figure 7B). Further depletion of FoxO3 markedly restored the metastatic dissemination of LM2 cells (Supplemental Figure 7A and Figure 7, A–C). Similarly, cosilencing Dicer significantly restored the metastatic potential of LM2 cells depleted of geminin or HDAC3 (Figure 7, D–F, and Supplemental Figure 7, C–F). These experiments underscore the importance of the FoxO3-Dicer axis as a central downstream effector mediating geminin/HDAC3-dependent promotion of breast cancer metastasis.

To evaluate the role of the molecular determinants for geminin/HDAC3/FoxO3 complex–binding specificity in controlling metastasis, we reconstituted geminin-depleted LM2 cells with WT or mutant geminin and compared their abilities in controlling metastasis. GEM^{WT}, but not the 2 binding defective mutants, restored the metastatic capacity in geminin-deficient LM2 cells (Figure, 7, G–I, and Supplemental Figure 7G). Analyzing rates of cell proliferation excluded their contributions to the altered meta-

static potential (Supplemental Figure 7H). Together, these results indicate that the actions of geminin on metastasis are largely dependent on its interactions with FoxO3 and HDAC3.

Negative correlation between geminin/HDAC3 and FoxO3 acetylation-Dicer in breast cancer. To explore the clinical implications of geminin-HDAC3-FoxO3-Dicer signaling and to assess its correlation with breast cancers, we performed immunohistochemical staining to examine the expression of these proteins in 183 cases of primary breast cancer samples. These tumor samples exhibited a positive correlation in the expression of Dicer and FoxO3 proteins, in contrast to an inverse correlation between Dicer and geminin or HDAC3 proteins (Figure 8A). In particular, the expression levels of geminin and HDAC3 were markedly elevated in breast cancer tissues, whereas Dicer levels were profoundly reduced. Meanwhile, aggressive breast cancers displayed significant, albeit modest, downregulation of FoxO3 (Figure 8A). None of these proteins showed promising correlation with the molecular subtypes of the breast cancer samples. Rather, these proteins were significantly correlated with the histological grades of the tumor samples (Supplemental Figure 8, A and B). qRT-PCR results using fresh-frozen breast tumor tissues revealed that the mRNA levels of *Dicer* in normal breast samples or ductal carcinoma in situ (DCIS) were approximately 6.3-fold higher than its levels in invasive ductal carcinoma (IDC) (Figure 8B). When the relative mRNA expression level of *Dicer* was plotted against that of FoxO3/geminin/HDAC3 in these fresh tissues, statistically significant correlations were visualized (Figure 8, C–E). Further evaluation of the prognostic significance of Dicer expression revealed that low Dicer levels were significantly correlated with poor overall survival rates in breast cancer patients (data obtained from PrognoScan, http://www.abren.net/PrognoScan/; Supplemental Figure 8C), suggesting that Dicer expression level is a potentially useful biomarker for prognosis prediction in patients with breast cancer. Of note, geminin gene copy number aberrations were not found in TCGA-derived breast cancer samples and the mRNA levels of *Dicer* showed no significant correlation with geminin mRNA levels in these samples (data obtained from the cBioPortal for Cancer Genomics, http://www.cbioportal.org/; Supplemental Figure 8D). Collectively, these results provide support for the clinical relevance of the functional interactions among these molecules.

To further validate the correlation among FoxO3 acetylation, Dicer expression, and geminin/HDAC3 protein levels in breast cancer samples, we extracted protein lysates from 3 normal breast tissues and 6 invasive breast cancers for acetyl-FoxO3 protein level analysis. Both acetyl-FoxO3 and Dicer protein expression were remarkably reduced in invasive tumors, whereas HDAC3 and geminin proteins were profoundly elevated in these samples (Figure 8F), supporting an inverse correlation between geminin/HDAC3 status and acetyl-FoxO3/Dicer levels. In contrast, c-Myc levels were unchanged in these samples. These results demonstrated that gain of geminin/HDAC3 facilitated FoxO3 deacetylation, which in turn shuts down Dicer transcription in breast cancers (Figure 8G).

Discussion

Dysregulation of geminin is often found in various types of human cancers. We report here that geminin promotes tumor invasion and metastasis by attenuating FoxO3-mediated transactivation of *Dicer*. The role of geminin in transcriptional repression has been demonstrated via its ability to form complexes with various transcription factors (20, 21). For instance, geminin has been reported to recruit HDAC3 via SMRT, thereby forming a transcriptional repressor complex with transcription factor AP4 (37). Unlike previous findings, our data revealed a direct interaction between geminin and HDAC3, which in turn tethered HDAC3 to FoxO3 for subsequent deacetylation. In contrast to its corepressor role in gene transcription, geminin has also been found to coactivate the transcription of neural genes via facilitating histone acetylation and increasing chromatin accessibility by unknown mechanisms. However, we failed to observe altered expression of acetyl-H3, acetyl-H4, acetyl-H3K9, or H3K27me3 in cells bearing ectopic geminin or depleted of geminin. The enrichment of these histone marks at the FoxO3 target promoters also remained unchanged, regardless of geminin expression levels in the cell, suggesting that repression of FoxO3-dependent gene transcription by geminin does not involve previously reported alterations of histone modifications. Geminin plays a crucial role in preventing DNA rereplication. The function of geminin in promoting metastasis is somewhat contradictory to its role as a "genome guard." We therefore investigated whether there is interplay between these two functional properties of geminin. Our results revealed that geminin's dual roles in DNA replication and in metastasis are in fact separate from each other. It is interesting to note that high levels of geminin protein have been reported in various human cancers. However, no aberrant geminin gene copy number was found in TCGA-derived breast cancer samples. Geminin is targeted for degradation by the anaphase-promoting complex (APC) during mitosis (16). It remains to be elucidated whether aberrant expression of geminin in human cancers is associated with impaired protein degradation machinery.

The influence of acetylation on the transcriptional activity of FoxO members remains a matter of debate. For both FoxO1 and FoxO3, 4 highly conserved lysine residues within their DBD are acetylated (11). Structural studies revealed that acetylation at some of these lysines decreases the DNA-binding affinity of FoxO proteins and subsequently compromises their transcriptional activity (42, 43). Consistent with this notion, several recent publications indicated that HDAC3-mediated deacetylation of FoxO proteins positively regulated their transcriptional activity (6, 38). For instance, increased FoxO1/FoxO3 acetylation due to impaired HDAC3 signaling resulted in attenuated miR-34c expression in glioblastoma cells (38). However, we failed to observe the regulation of miR-34c by FoxO3 in breast cancer cells, suggesting this regulation might be tissue specific. This context-dependent regulation of a downstream target gene by FoxO has been discussed by other groups recently. One example is *P27*, which has been widely used as a FoxO target gene. However, in *Foxo* triple knockout (TKO) mice, only thymocytes showed diminished p27 expression (44). These studies suggest that FoxOs regulate gene transcription in a tissue-specific manner in general. In agreement with previous findings that acetylation promotes FoxO-mediated transcription (7, 45), we found that HDAC3 depletion in breast cancer cells activated FoxO3-dependent gene transcription. In FoxO3-depleted cells, the acetylation-mimic mutant FoxO3^{5KQ},

but not the acetylation-deficient mutant $FoxO3_{5KR}$, profoundly restored expression levels of FoxO3 targets, further supporting the notion that FoxO3 acetylation activates gene transcription. Moreover, previous studies have revealed that different FoxO-responsive targets can respond differently to the presence of SIRT1 (7). Therefore, the impact of acetylation/deacetylation on the transcriptional activity of FoxO members can be promoter context dependent. Furthermore, we speculate that, similarly to the mode of acetylation-dependent regulation of p53, distinct acetylation sites of FoxOs may control promoter-specific activation of FoxO targets and are therefore differentially required for diverse cellular functions of FoxO members. It has been proposed that p53 K120 acetylation is critical for p53-mediated apoptosis, but has no effect on p53-dependent cell-cycle arrest (46). In contrast, $p53^{3KR}$ (K117R+K161R+K162R) lost the ability to induce cell-cycle arrest, apoptosis, and senescence, but retained the capacity to regulate energy metabolism and ROS production (47). These studies highlight that acetylation/deacetylation at the selected lysine residues may add an additional layer of regulation when nonhistone proteins are subjected to such modification. Additionally, when FoxOs form multiprotein complexes with deacetylases such as HDAC3, the effect of deacetylation on FoxO-mediated gene transcription might be coordinated by the whole complex, rather than by the deacetylase itself. It has been suggested that lysine acetylation has a significant impact on protein-protein interactions. For instance, Wang et al. (48) recently showed that the interaction between p53 and SET occurs in an acetylation-dependent manner. The p53 acetylation at its C-terminal domain (CTD) disrupted this interaction, allowing p300 to regulate histone acetylation at p53 target promoters. Likewise, the acetylation status of FoxO3 may serve as a key determinant in multiprotein complex formation under certain biological settings, which ultimately influences FoxO3-directed gene transcription. Taking these data together, it is plausible that HDAC-mediated deacetylation may exert dual effects on distinct lysine residues and that, once acetylated or deacetylated, the binding affinity of FoxOs with DNA is fine-tuned by multiple factors rather than by acetylation/deacetylation per se.

Although the DBDs of both FoxO3 and FoxO1 are highly conserved, sequence conservation outside the DBD is very low. We found that the hypervariable N-terminal domains of these 2 family members determines their geminin-binding specificity, thereby favoring the formation of the geminin-FoxO3 complex in cells. Further analysis revealed that preferential binding of geminin to FoxO3 derived from nonconserved residues 100–120 of FoxO3. This distinct binding affinity in turn led to selective deacetylation of FoxO3 mediated by the association between geminin and HDAC3. Meanwhile, geminin deficiency is unable to further increase Dicer expression in HDAC3 knockdown cells, arguing that HDAC3 is indispensable for the inhibition of FoxO3 by geminin. We further demonstrated that this enzyme substrate coupling property of geminin underlies its oncogenic function, promoting tumor invasion and metastatic dissemination by repressing FoxO3-mediated transactivation of *Dicer*.

The fact that FoxO3 is a pivotal regulator in stress response and cellular homeostasis led us to postulate that geminin may be involved in a broad range of cell functions through modulation of FoxO3 transcriptional activity. Interestingly, both geminin and FoxO3 have been implicated in regulating the homeostasis of the hematopoietic and immune systems (49–51). It remains to be elucidated whether the actions of geminin in controlling cellular homeostasis in response to pathophysiological stimuli require FoxO3. The identification of Dicer as a new downstream target of FoxO3, mediating its role in breast cancer metastasis, is intriguing. Consistent with this finding, array expression profiling analyses have revealed a global reduction of miRNA expression in cells depleted of FoxO3. Adding back Dicer profoundly restored expression levels of a subset of miRNAs in FoxO3 knockdown cells, suggesting that FoxO3 may act on Dicer to regulate the biosynthesis of miRNA. Lower Dicer expression was found to be associated with advanced tumor stages and poor clinical outcome in various human cancers (52, 53). Indeed, Dicer levels were remarkably decreased in grade III as well as the invasive breast cancers, which inversely correlated with elevated geminin and/or HDAC3 levels. Of note, the concurrent downregulation of acetyl-FoxO3 was observed in the invasive breast cancers, supporting our conclusion that the aberrant accumulation of geminin/HDAC3 in aggressive breast cancers may suppress FoxO3-dependent Dicer expression via promotion of its deacetylation (Figure 8G) and further underscoring the essential roles of these proteins during breast cancer progression.

Methods

Cell culture. HEK-293T, MCF-7, MDA-MB-231, HCT116, MCF-10A, and 3T3-L1 cell lines were originally obtained from ATCC; LM2 cells were a gift from Guohong Hu (Institute of Health Sciences, Shanghai, China). MEF cells were generated as described (8). HEK-293T, MCF-7, MDA-MB-231, LM2, MEF, and 3T3-L1 cells were cultured in DMEM (Gibco, Thermo Fisher Scientific) supplemented with 10% FBS. HCT116 cells were cultured in McCoy's 5A (Thermo Fisher Scientific) supplemented with 10% FBS. MCF-10A cells were maintained in DMEM/F12 medium with 5% horse serum, 10 ng/ml human EGF, 500 ng/ml hydrocortisone, and 100 ng/ml bovine insulin. All cells were maintained at 37°C in a saturated humidity atmosphere containing 95% air and 5% CO_2.

Luciferase assays. Luciferase reporter assay was performed as described previously (33). Briefly, the reporter constructs were cotransfected into HEK293T cells using a calcium phosphate transfection method with different expression vectors and internal control plasmid (β-gal). Luciferase assays were performed using the same amount of cell extracts and corrected for transfection efficiency using internal controls (β-gal). All samples were analyzed in triplicate.

GST pull-down assay. GST fusion constructs were expressed in BL21, and crude bacterial lysates were prepared by sonication in cold NETN buffer (50 mM Tris-HCl pH 8.0, 120 mM NaCl, 1 mM EDTA, pH 8.0, 0.5% NP-40) in the presence of the protease inhibitor mixture. Then GST fusion proteins were purified by glutathione-Sepharose beads. In GST pull-down assays, about 10 μg of the appropriate GST fusion proteins were mixed with cell lysates or purified proteins. The binding reaction was mixed at 4°C for 2 hours. The beads were washed 5 times with NETN or cell lysis buffer (50 mM Tris-HCl, pH 8.0, 100 mM NaCl, 40 mM β-glycerol phosphate, 1 mM Na_4VO_3, 10 mM NaF, 1% Triton X-100), resuspended in 15 μl of 2× SDS-PAGE loading buffer, and resolved on the appropriate Tris-Glycine gel. Protein bands were detected with specific antibodies by Western blotting.

Acetylation assessment. Cultured cells or snap-frozen tissue samples were lysed and homogenized with acetylation assessment lysis buffer (20 mM Tris-HCl, pH 7.5, 150 mM NaCl, 1 mM EDTA, 1 mM EGTA, 1% Triton X-100, 50 mM NaF, 5 mM β-glycerol phosphate, 1 mM Na_3VO_4, 5 mM TSA, and 10 mM nicotinamide). Protein concentration of each sample was determined using the BCA Kit (Pierce, 23235) per the manufacturer's instructions. Equal amounts of protein extracts were immunoprecipitated with anti-FoxO1/3 or anti–acetylated-Lys. The immunoprecipitates were then separated by electrophoresis on Tris-Glycine gels.

ChIP assay and ChIP-ReChIP. Cells were treated with formaldehyde to create protein-DNA crosslinks, and the crosslinked chromatin was extracted and sheared by sonication. Protein A/G beads were precleared and blocked with 1% salmon sperm DNA and 1% BSA. Total sheared chromatin was used for immunoprecipitation with either normal rabbit/mouse/goat IgG, FoxO3 (Santa Cruz Biotechnology Inc., catalog 11351), geminin (Santa Cruz Biotechnology Inc., catalog 8448), or HDAC3 (Cell Signaling Technology, catalog 3949) antibody. The immunoprecipitates were washed 5 times, pelleted by centrifugation, and then heated at 65°C for 4 hours to decrosslink. For ChIP-ReChIP, DNA-protein complexes were washed 5 times, eluted with 10 mM DTT at 37°C for 30 minutes, and resubjected to immunoprecipitation. The immunoprecipitates were washed, eluted, and decrosslinked. After proteins and RNA were degraded by treatment with proteinase K, DNA was purified. Amplified PCR products were analyzed using agarose gel electrophoresis, followed by quantification. Primer sequences used for ChIP experiments are listed in Supplemental Table 4.

RNA sequencing and data deposition. Total RNA was isolated with TRIzol reagents following the manufacturer's instructions (Invitrogen). cDNA library construction and illumine HiSeq4000 sequencing were conducted at Novogene. All original microarray data were deposited in the NCBI's Gene Expression Omnibus (GEO GSE94687).

Immunofluorescence. LM2 cells grown in 10-cm^2 dishes were transfected with HA-FoxO3 (2 μg). Twenty-four hours later, cells were split into new 10-cm^2 dishes with coverslips. Another 24 hours later, the culture medium was removed and coverslips were carefully washed 3 times with PBS. Then cells were fixed with 4% paraformaldehyde for 5 minutes at room temperature and subsequently washed twice with PBS and twice with washing buffer. Cells were then permeabilized for 5 minutes with 0.5% Triton X-100, blocked in PBS plus 1% BSA, and subsequently incubated with anti-HDAC3, anti-geminin, or anti-FLAG antibodies at 4°C overnight. After washing 3 times with PBS, the cells were incubated with Alexa Fluor 488 donkey anti-mouse IgG (Life Technologies, A21202), Alexa Fluor 568 goat anti-rabbit IgG (Life Technologies, A11036), and Alexa Fluor 647 donkey anti-goat IgG (Life Technologies, A21447) at room temperature for 1 hour in the dark. After extensive washing with ice-cold PBS, the nuclei were counterstained with DAPI for 10 minutes. Then specimens were mounted in 90% glycerol and sealed with nail polish. Confocal fluorescence images were obtained with a confocal microscope (LSM 780 NLO, Carl Zeiss).

Immunohistochemistry. Formalin-fixed paraffin-embedded 5-μm tissue sections were deparaffinized in xylenes and rehydrated through a graded series of alcohols. After antigen retrieval was performed, all sections were blocked at room temperature in avidin/biotin blocking buffer (Vector Laboratories) and then 3% BSA for 30 minutes. Staining with antibodies was conducted at room temperature for 60 minutes. Sections were rinsed twice in PBS, and protein staining was performed using an diaminobenzidine (DAB) substrate kit (Maixin Biotech, KIT-9710). Samples were counterstained with hematoxylin. Immunohistochemistry images were obtained using an upright microscope (Olympus BX51). Brown staining indicated the immunoreactivity of samples.

Migration/invasion assay. For in vitro migration assay, an 8-μm pore size Boyden chamber (Corning Costar, 3422) was used. Cells (100 μl, 1×10^5) in 0.5% serum-containing DMEM were plated in the upper chamber, and 600 μl 10% FBS was added to DMEM in the lower chamber as a chemoattractant. For invasion assay, an 8-μm pore size BD Matrigel Invasion Chamber was used. After 4 hours (MDA–MB-231 and LM2) or 72 hours (MCF-7) for migration assay and 8 hours (MDA–MB-231 and LM2) or 144 hours (MCF-7) for invasion assay, cells on the upper side of the filter were removed and cells that remained adherent to the underside of membranes were fixed in formaldehyde, followed by staining with crystal violet. The number of migrated cells was counted using a microscope. Five contiguous fields of each sample were examined using a 20× objective to obtain a representative number of cells that migrated/invaded across the membrane.

Animal studies. Six-week-old Balb/c nude mice were used for all studies. For metastasis formation, cells were harvested, washed twice in PBS, counted, and then resuspended in a 1:1 solution of PBS and Matrigel Matrix (Corning, 356231). Mice were anesthetized, a small incision was made to reveal the no. 4 mammary fat pad, and luciferase-labeled cells (3×10^6 for MDA–MB-231, 10^6 for LM2 cells, and 10^7 for MCF-7 cells) were injected directly into the mammary fat pad. For MCF-7 metastasis assay, nude mice were preimplanted subcutaneously with 1.7 mg of 17 β-estradiol pellets (60-day release; Innovative Research of America). When tumors became palpable, tumor volume was assessed by caliper measurements using the following formula: π (width^2 × length)/6 (mm^3). The tumors were extracted from mammary glands when they reached 300 mm^3. Seven days after tumor removal, mice were monitored by bioluminescent imaging for the development of metastases.

Bioluminescent imaging and analysis. Mice were anesthetized and injected with 1.5 mg of D-luciferin (15 mg/ml in PBS). Imaging was completed between 2 and 5 minutes after injection with a Xenogen IVIS Lumina system coupled to Living Image acquisition and analysis software (Xenogen). Images were analyzed with Living Image software ver. 3.0. Bioluminescent flux (photons/s/cm^2/steradian) was determined for the mouse in a prone position.

For additional information, see Supplemental Methods.

Statistics. Results are reported as mean ± SD of 3 or more independent experiments. ANOVA was used to compare among groups, whereas Student's *t* test was used to determine significance between groups. All *P* values reported are 2 sided unless otherwise noted. $P < 0.05$ was considered statistically significant. Statistical analyses were performed with GraphPad Prism 5 software.

Study approval. Prior to obtaining patient samples, requisite approval from the Medical Ethics Committee of the First Affiliated Hospital of Xiamen University and written informed consent from the patients were obtained. The mouse experiments were approved by the Institutional Animal Care and Use Committee of Xiamen University.

Author contributions

This project was conceived and supervised by HY. The experiments were designed by HY and LZ. Most of the experiments were per-

formed by LZ and MC. Some experiments were supervised by ZG, BZ, YL, LG, XH, QL, GL, MHY, and YEC. The breast cancer sample collection and immunohistochemical analysis were contributed by JY and ZX. The manuscript was prepared by LZ, YEC, and HY.

Acknowledgments

We thank Zhongxian Lv for helping with Bioluminescent Imaging and Wei Xie, Yang Mei, and Huihui Liu for excellent technical support. This work was supported by National Natural Science Foundation of China grant U1505223 (to HY), the National Program on Key Research Project 2016YFC 1302400 (to HY), National Basic Research Program of China 973 program grant 2015CB553802 (to HY), National Natural Science Foundation of China grants 81372619 (to HY) and 31300627 (to LZ), Fundamental Research Funds for the Central Universities grants 20720150066 (to HY) and 20720150059 (to LZ), and the 111 Project of the Ministry of Education of China (B06016).

Address correspondence to: Han You, School of Life Sciences, Xiamen University, Xiang'an Nan Road, Xiang'an District, Xiamen 361102, Fujian, China. Phone: 0086.0592.2180113; E-mail: hyou@xmu.edu.cn.

1. Norris KL, Lee JY, Yao TP. Acetylation goes global: the emergence of acetylation biology. *Sci Signal*. 2009;2(97):pe76.
2. Yang XJ, Seto E. Lysine acetylation: codified crosstalk with other posttranslational modifications. *Mol Cell*. 2008;31(4):449–461.
3. Yang XJ, Seto E. The Rpd3/Hda1 family of lysine deacetylases: from bacteria and yeast to mice and men. *Nat Rev Mol Cell Biol*. 2008;9(3):206–218.
4. Hassig CA, Fleischer TC, Billin AN, Schreiber SL, Ayer DE. Histone deacetylase activity is required for full transcriptional repression by mSin3A. *Cell*. 1997;89(3):341–347.
5. Laherty CD, Yang WM, Sun JM, Davie JR, Seto E, Eisenman RN. Histone deacetylases associated with the mSin3 corepressor mediate mad transcriptional repression. *Cell*. 1997;89(3):349–356.
6. Mihaylova MM, et al. Class IIa histone deacetylases are hormone-activated regulators of FOXO and mammalian glucose homeostasis. *Cell*. 2011;145(4):607–621.
7. Brunet A, et al. Stress-dependent regulation of FOXO transcription factors by the SIRT1 deacetylase. *Science*. 2004;303(5666):2011–2015.
8. You H, et al. FOXO3a-dependent regulation of Puma in response to cytokine/growth factor withdrawal. *J Exp Med*. 2006;203(7):1657–1663.
9. Eijkelenboom A, Burgering BM. FOXOs: signalling integrators for homeostasis maintenance. *Nat Rev Mol Cell Biol*. 2013;14(2):83–97.
10. Greer EL, Brunet A. FOXO transcription factors at the interface between longevity and tumor suppression. *Oncogene*. 2005;24(50):7410–7425.
11. Calnan DR, Brunet A. The FoxO code. *Oncogene*. 2008;27(16):2276–2288.
12. Furuyama T, et al. Abnormal angiogenesis in Foxo1 (Fkhr)-deficient mice. *J Biol Chem*. 2004;279(33):34741–34749.
13. Hosaka T, et al. Disruption of forkhead transcription factor (FOXO) family members in mice reveals their functional diversification. *Proc Natl Acad Sci U S A*. 2004;101(9):2975–2980.
14. Castrillon DH, Miao L, Kollipara R, Horner JW, DePinho RA. Suppression of ovarian follicle activation in mice by the transcription factor Foxo3a. *Science*. 2003;301(5630):215–218.
15. Zhang Y, et al. Regulation of cell cycle progression by forkhead transcription factor FOXO3 through its binding partner DNA replication factor Cdt1. *Proc Natl Acad Sci U S A*. 2012;109(15):5717–5722.
16. McGarry TJ, Kirschner MW. Geminin, an inhibitor of DNA replication, is degraded during mitosis. *Cell*. 1998;93(6):1043–1053.
17. Wohlschlegel JA, Dwyer BT, Dhar SK, Cvetic C, Walter JC, Dutta A. Inhibition of eukaryotic DNA replication by geminin binding to Cdt1. *Science*. 2000;290(5500):2309–2312.
18. Zhu W, Depamphilis ML. Selective killing of cancer cells by suppression of geminin activity. *Cancer Res*. 2009;69(11):4870–4877.
19. Kroll KL, Salic AN, Evans LM, Kirschner MW. Geminin, a neuralizing molecule that demarcates the future neural plate at the onset of gastrulation. *Development*. 1998;125(16):3247–3258.
20. Del Bene F, Tessmar-Raible K, Wittbrodt J. Direct interaction of geminin and Six3 in eye development. *Nature*. 2004;427(6976):745–749.
21. Luo L, Yang X, Takihara Y, Knoetgen H, Kessel M. The cell-cycle regulator geminin inhibits Hox function through direct and polycomb-mediated interactions. *Nature*. 2004;427(6976):749–753.
22. Seo S, Kroll KL. Geminin's double life: chromatin connections that regulate transcription at the transition from proliferation to differentiation. *Cell Cycle*. 2006;5(4):374–379.
23. Patterson ES, Waller LE, Kroll KL. Geminin loss causes neural tube defects through disrupted progenitor specification and neuronal differentiation. *Dev Biol*. 2014;393(1):44–56.
24. Sato K, et al. Contrast-enhanced intraoperative ultrasonography for vascular imaging of hepatocellular carcinoma: clinical and biological significance. *Hepatology*. 2013;57(4):1436–1447.
25. Bravou V, Nishitani H, Song SY, Taraviras S, Varakis J. Expression of the licensing factors, Cdt1 and Geminin, in human colon cancer. *Int J Oncol*. 2005;27(6):1511–1518.
26. Blanchard Z, et al. Geminin overexpression induces mammary tumors via suppressing cytokinesis. *Oncotarget*. 2011;2(12):1011–1027.
27. Gonzalez MA, et al. Geminin predicts adverse clinical outcome in breast cancer by reflecting cell-cycle progression. *J Pathol*. 2004;204(2):121–130.
28. Caronna EA, Patterson ES, Hummert PM, Kroll KL. Geminin restrains mesendodermal fate acquisition of embryonic stem cells and is associated with antagonism of Wnt signaling and enhanced polycomb-mediated repression. *Stem Cells*. 2013;31(8):1477–1487.
29. Emmett LS, O'Shea KS. Geminin is required for epithelial to mesenchymal transition at gastrulation. *Stem Cells Dev*. 2012;21(13):2395–2409.
30. Harfe BD, McManus MT, Mansfield JH, Hornstein E, Tabin CJ. The RNaseIII enzyme Dicer is required for morphogenesis but not patterning of the vertebrate limb. *Proc Natl Acad Sci U S A*. 2005;102(31):10898–10903.
31. Minn AJ, et al. Genes that mediate breast cancer metastasis to lung. *Nature*. 2005;436(7050):518–524.
32. Saxena S, et al. A dimerized coiled-coil domain and an adjoining part of geminin interact with two sites on Cdt1 for replication inhibition. *Mol Cell*. 2004;15(2):245–258.
33. Mei Y, et al. Regulation of neuroblastoma differentiation by forkhead transcription factors FOXO1/3/4 through the receptor tyrosine kinase PDGFRA. *Proc Natl Acad Sci U S A*. 2012;109(13):4898–4903.
34. Lee YS, et al. Distinct roles for Drosophila Dicer-1 and Dicer-2 in the siRNA/miRNA silencing pathways. *Cell*. 2004;117(1):69–81.
35. Liu Q, et al. R2D2, a bridge between the initiation and effector steps of the Drosophila RNAi pathway. *Science*. 2003;301(5641):1921–1925.
36. Spellberg MJ, Marr MT. FOXO regulates RNA interference in Drosophila and protects from RNA virus infection. *Proc Natl Acad Sci U S A*. 2015;112(47):14587–14592.
37. Kim MY, et al. A repressor complex, AP4 transcription factor and geminin, negatively regulates expression of target genes in nonneuronal cells. *Proc Natl Acad Sci U S A*. 2006;103(35):13074–13079.
38. Masui K, et al. mTOR complex 2 controls glycolytic metabolism in glioblastoma through FoxO acetylation and upregulation of c-Myc. *Cell Metab*. 2013;18(5):726–739.
39. Yellajoshyula D, Patterson ES, Elitt MS, Kroll KL. Geminin promotes neural fate acquisition of embryonic stem cells by maintaining chromatin in an accessible and hyperacetylated state. *Proc Natl Acad Sci U S A*. 2011;108(8):3294–3299.
40. Martello G, et al. A MicroRNA targeting dicer for metastasis control. *Cell*. 2010;141(7):1195–1207.
41. Melixetian M, et al. Loss of Geminin induces rereplication in the presence of functional p53. *J Cell Biol*. 2004;165(4):473–482.
42. Matsuzaki H, Daitoku H, Hatta M, Aoyama H, Yoshimochi K, Fukamizu A. Acetylation of Foxo1 alters its DNA-binding ability and sensitivity to phosphorylation. *Proc Natl Acad Sci U S A*. 2005;102(32):11278–11283.
43. Tsai KL, Sun YJ, Huang CY, Yang JY, Hung MC, Hsiao CD. Crystal structure of the human FOXO3a-DBD/DNA complex suggests the effects of post-translational modification. *Nucleic*

Acids Res. 2007;35(20):6984–6994.
44. Paik JH, et al. FoxOs are lineage-restricted redundant tumor suppressors and regulate endothelial cell homeostasis. *Cell*. 2007;128(2):309–323.
45. Motta MC, et al. Mammalian SIRT1 represses forkhead transcription factors. *Cell*. 2004;116(4):551–563.
46. Tang Y, Zhao W, Chen Y, Zhao Y, Gu W. Acetylation is indispensable for p53 activation. *Cell*. 2008;133(4):612–626.
47. Li T, et al. Tumor suppression in the absence of p53-mediated cell-cycle arrest, apoptosis, and senescence. *Cell*. 2012;149(6):1269–1283.
48. Wang D, et al. Acetylation-regulated interaction between p53 and SET reveals a widespread regulatory mode. *Nature*. 2016;538(7623):118–122.
49. Karamitros D, et al. Differential geminin requirement for proliferation of thymocytes and mature T cells. *J Immunol*. 2010;184(5):2432–2441.
50. Miyamoto K, et al. Foxo3a is essential for maintenance of the hematopoietic stem cell pool. *Cell Stem Cell*. 2007;1(1):101–112.
51. Tothova Z, et al. FoxOs are critical mediators of hematopoietic stem cell resistance to physiologic oxidative stress. *Cell*. 2007;128(2):325–339.
52. Faggad A, et al. Prognostic significance of Dicer expression in ovarian cancer-link to global microRNA changes and oestrogen receptor expression. *J Pathol*. 2010;220(3):382–391.
53. Jafarnejad SM, Ardekani GS, Ghaffari M, Martinka M, Li G. Sox4-mediated Dicer expression is critical for suppression of melanoma cell invasion. *Oncogene*. 2013;32(17):2131–2139.